JACS
JOURNAL OF THE AMERICAN CHEMICAL SOCIETY

Communication

pubs.acs.org/JACS

Two Different Structures of the Oxygen-Evolving Complex in the Same Polypeptide Frameworks of Photosystem II

Ayako Tanaka,[†] Yoshimasa Fukushima,[‡] and Nobuo Kamiya*[,†,‡]

[†]Department of Chemistry, Graduate School of Science, Osaka City University, 3-3-138 Sugimoto, Sumiyoshi, Osaka 558-8585, Japan
[‡]The OCU Advanced Research Institute for Natural Science and Technology (OCARINA), Osaka City University, 3-3-138 Sugimoto, Sumiyoshi, Osaka 558-8585, Japan

Supporting Information

ABSTRACT: The oxygen-evolving complex (OEC) forms the heart of photosystem II (PSII) in photosynthesis. The crystal structure of PSII from *Thermosynechococcus vulcanus* has been reported at a resolution of 1.9 Å and at an averaged X-ray dose of 0.43 MGy. The OEC structure is suggested to be partially reduced to Mn(II) by EXAFS and DFT computational studies. Recently, the "radiation-damage-free" structures have been published at 1.95 Å resolution using XFEL, but reports continued to appear that the OEC is reduced to the S_0-state of the Kok cycle. To elucidate much more precise structure of the OEC, in this study two structures were determined at extremely low X-ray doses of 0.03 and 0.12 MGy using conventional synchrotron radiation source. The results indicated that the X-ray reduction effects on the OEC were very small in the low dose region below 0.12 MGy, that is, a threshold existed for the OEC structural changes caused by X-ray exposure. The OEC structures of the two identical monomers in the crystal were clearly different under the threshold of the radiation dose, although the surrounding polypeptide frameworks of PSII were the same. The assumption that the OECs in the crystal were in the dark-stable S_1-state of the Kok cycle should be re-evaluated.

Photosystem II (PSII) is a multisubunit protein complex embedded in the thylakoid membrane and splits water molecules, producing electrons, protons and molecular oxygen in photosynthesis.[1,2] Crystal structures of PSII from *Thermosynechococcus elongatus* and *Thermosynechococcus vulcanus* have been reported,[3−8] which are highly informative for understanding how PSII conducts energy transfer, light-induced charge separation, electron transfer, and oxygen-evolving reactions, including proton transfer. PSII exists in the asymmetric unit of the crystal as a homodimer, and each monomer is defined as the A- and B-monomer, respectively (see the Supporting Information and Figure S1). The oxygen-evolving complex (OEC) in PSII acts as a catalyst according to the Kok's S_i-state model (i = 0−4),[1] and the OEC structure was determined precisely by X-ray crystallography at a resolution of 1.9 Å[7] (the structure of PDB-ID: 3WU2, partially revised from the initial 3ARC, is named as Native_0.43MGy in this paper) on the assumption that the OECs in the crystal were in the dark-stable S_1-state, because the PSII crystals used for the diffraction experiments were stored in the dark during crystallization and during the diffraction intensity measurements. The diffraction data set had been collected at an averaged X-ray dose of 0.43 MGy (0.85 MGy indicated in the previous literature[7] was the final dose in total for one data collection). Extended X-ray absorption fine structure (EXAFS) studies suggested that the OEC structure in Native_0.43MGy was partially affected by X-ray reduction to Mn(II) atoms.[9−12] EXAFS and computational studies indicated that the structures included the S_0-state in the Kok cycle or further reduced states.[13,14] Recently, an X-ray free-electron laser (XFEL) was used to collect diffraction data from PSII crystals and the "radiation-damage-free" structures were published (the structures of PDB-IDs, 4UB6 and 4UB8, are referred as XFEL-1 and XFEL-2 in this paper),[15] but reports continued to appear that the OEC is reduced to the S_0-state.[16,17] In fact, some abnormal characters were found on the temperature factors of calcium (Ca) atoms in the OEC of the XFEL structures (see later). On the other hand, the EXAFS study by Glockner et al.[11] at a low dose (5% Mn reduction) showed that the EXAFS data of the S_0*-state induced by X-ray exposure did not match with that for the physiologically relevant S_0-state. In order to obtain much more precise information for the intact structure of the OEC, in this study two structures (LowDose-1 and LowDose-2) were determined with highly reliable diffraction data sets of 1.87 and 1.85 Å resolutions, collected at 100 K using the conventional synchrotron radiation source at extremely low X-ray doses, one each at 0.03 and 0.12 MGy. The value of 0.03 MGy (less than 1% Mn reduction) is only 1.5 times larger than the X-ray dose used to measure the intact absorption edge spectra at 10 K in the previous EXAFS studies.[9] Furthermore, the absorption edge profile of the PSII crystals used in this study was measured at an X-ray dose of 0.01 MGy (see Supporting Information and Figure S2). The profile of the crystal sample and the energy shift of the profile from 10 mM $MnCl_2$ solution were almost the same, with the results presented for the intact PSII crystal in Figure 1 of the literature.[9] Thus, the two PSII structures reported here (PDB-IDs; 5B5E and 5B66) are expected to show the intact or nearly intact OEC structures, which will be very important in order to discuss the oxygen-evolving mechanism of PSII.

The averaged X-ray dose was reduced in this study by using many PSII crystals highly isomorphous (see Supporting

Received: September 19, 2016
Published: January 19, 2017

DOI: 10.1021/jacs.6b09666
J. Am. Chem. Soc. 2017, 139, 1718−1721

Information). The quality of the structure determination is indicated in Figure 1a by showing electron density distributions

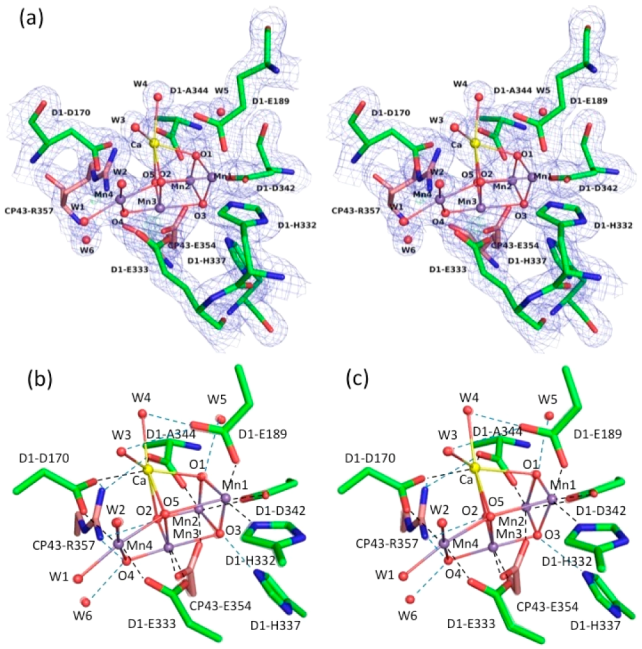

Figure 1. Structures of the oxygen-evolving complex in photosystem II. (a) Stereodrawing of the OEC model in the A-monomer obtained using a data set of LowDose-1 at 0.03 MGy and the $2|F_o| - |F_c|$ electron density map at the 1.0σ level. (b) Structure models of the A-monomer of LowDose-1 are superposed on those of LowDose-2 at 0.12 MGy (faded colors). (c) Structure models of the B-monomer of LowDose-1 are drawn on those of LowDose-2 in the same manner to (b). Root-mean-squares deviations are calculated as 0.08 Å for both of the Mn_4CaO_5 clusters in panels b and c. Broken lines in black and blue indicate the valence bonds and the hydrogen bonds, respectively.

around the OEC of the A-monomer in the LowDose-1 structure (see Figure S3 for the B-monomer). Due to the higher qualities of the data sets (Table S1) compared to Native_0.43MGy, clear electron density distributions are observed as shown in Figure S4 around the oxo-bridging oxygen atoms (O1−O5) and the water molecules directly ligated to the metal ions (W1−W4). The restrained least-squares refinements were completed with reasonable statistics (see Supporting Information and Table S2) and the overall polypeptide frameworks of PSII are very similar to each other and with Native_0.43MGy. We superposed the two corresponding monomers from the LowDose-1 and LowDose-2 structures using the polypeptide Cα atoms of D1 (Phe17-Ser222 and Ser268-A344) and D2 (Gly34-Thr221 and Thr243-Leu352) subunits, as shown in Figures 1b,c. Both of the two superposed OEC structures were very similar, despite the different X-ray doses (0.03 and 0.12 MGy).

The atomic distances between two metal ions and those between each of the metal ions and its ligand atoms in the OECs are compared in Figures S5 and S6, respectively, and their numerical values are listed in Tables S3 and S4 including the two structures of XFEL-1 and XFEL-2 resolved using XFEL.[15] The atomic distances in the OEC of Native_0.43MGy tended to be longer than those of the LowDose-1 and LowDose-2 structures, indicative of structural changes in the OEC caused by X-ray reduction, whereas the distances in the two structures at low doses were highly similar. Furthermore, the metal−metal distances were also similar to the XFEL "radiation-damage-free" structures, with an error range of 0.1 Å except having significantly small temperature factors of Ca, W3, and W4 directly ligated to the Ca atom, and W5 nearest to the Ca atom, compared with XFEL-1 and XFEL-2 (Table S5). If the Mn atoms in the OECs of the two XFEL structures were reduced by X-ray exposure, the temperature factors of the four Mn atoms should be increased. But they were similar to the values of LowDose-1 and LowDose-2 as listed in Table S5. On the basis of the fact, we concluded that the OEC structures of XFEL-1 and XFEL-2 were not affected by the X-ray reduction. Generally, the temperature factors of atoms in the Mn_4CaO_5 clusters defined as one group in the restrained least-squares refinement are similar to each other as the case of side changes of amino acid residues, which are also defined as the groups in the restrained least-squares refinement. One exception is that the amino acid side chains have highly disordered structures, in which the temperature factors of atoms increase dramatically toward the ends of the side chains. In the A-monomers of the two XFEL structures, W 5s (HOH601/A of XFEL-1 and HOH602/A of XFEL-2) are located at similar positions with those in LowDose-1 and LowDose-2, but in the B-monomers the water molecules (HOH561/a of XFEL-1 and HOH560/a of XFEL-2) exist at different sites. The distances between the new sites and W 4s are 2.61 and 2.41 Å in the two XFEL structures and 3.59 and 3.45 Å in LowDose-1 and LowDose-2, respectively. Furthermore, the distances between the new sites and O 1s are 2.43 and 2.45 Å in the XFEL structures. The corresponding distances are 2.74 Å in LowDose-1 and 2.69 Å in LowDose-2, which are within the range of hydrogen bonds. Because the very short distances found around the new sites in the XFEL structures resemble to the Ca−water distances, not to the water−water ones, it can be speculated that the Ca atoms in the OECs are disordered at the initial site and at the new site assigned as the water molecules (HOH561/a and HOH560/a) in the XFEL structures.

As mentioned above, X-ray reductions of the Mn atoms in the OEC at doses above 0.43 MGy (12% Mn reduction) result in elongation of the atomic distances in the OEC. Contrary, the X-ray reduction induces very small differences at doses below 0.12 MGy. The OEC structures in LowDose-1 at 0.03 MGy (less than 1% Mn reduction) and in LowDose-2 at 0.12 MGy (3.5% Mn reduction) have possibilities to be a mixture of the S_1- and S_0-states, and that of the S_1-state and the S_0*-state reduced by X-ray exposure (5% Mn reduction).[11] The structural changes in the OEC between the S_1- and S_0-states or between the S_1- and S_0*-states may be smaller than the distance error of 0.1 Å estimated in this study (see Supporting Information).

When the OECs of the two monomers in the LowDose-1 structure were superposed, as shown in Figure 2, differences in the OEC structures of the two monomers were clearly evident. Many bond shortenings and elongations were observed (Tables S3 and S4), and here the two hydrogen bonds between O3 and D1-His337 and between O4 and W6 were noteworthy. The hydrogen-bond distance between O3 and D1-His337 was shortened from 2.75 Å in the B-monomer to 2.46 Å in the A-monomer. The shortening of 0.29 Å (reliability-1:97.2%, calculated with the error value of 0.1 Å as the standard deviation, the 1σ level) was synchronized with an elongation of 0.31 Å at the O3−Mn3 bond from 1.96 to 2.27 Å. In contrast, the hydrogen-bond distance between O4 and W6 was elongated from 2.44 Å in the B-monomer to 2.66 Å in the A-

DOI: 10.1021/jacs.6b09666
J. Am. Chem. Soc. 2017, 139, 1718−1721

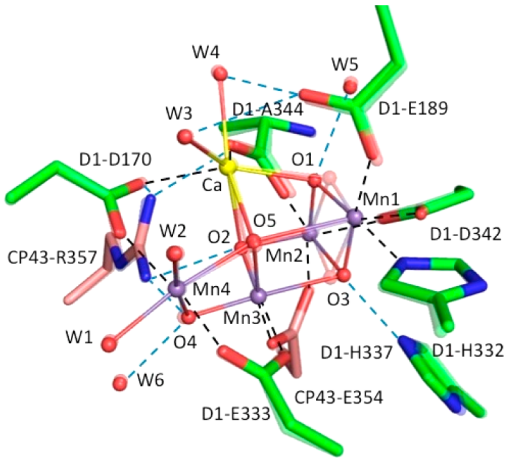

Figure 2. Superposition of structures around the OECs in the A- and B-monomers obtained using a data set of LowDose-1 at 0.03 MGy. The structures for the B-monomer are represented with faded colors. The root-mean-square deviation is calculated as 0.21 Å for the Mn_4CaO_5 cluster. Broken lines in black and blue indicate the valence bonds and the hydrogen bonds, respectively.

monomer. The elongation of 0.22 Å (reliability-2:88.0%) was accompanied by the 0.20 Å shortening of the O4−Mn4 bond from 2.07 to1.87 Å. The two values of reliability-1 and -2 were not extremely high comparing with 99.7% of the 3σ level. Because the shortening and elongation of the hydrogen bonds occurred simultaneously in one OEC, the joint reliability (defined as reliability-1 + reliability-2 − reliability-1 × reliability-2) for the two distance changes was calculated to be over 99.7%, and was sufficiently high to judge that the two OEC structures in the PSII crystal were different.

The two identical monomers (A and B) in the asymmetric unit in the crystal exhibited two structures of the OEC with the different hydrogen-bonding patterns as mentioned above. The OEC structures may be affected by differences in the packing environments around the two monomers in the crystal. The packing effects would be very small because the OECs are buried deep inside PSII (the minimum distances from the OEC in the A-monomer to the surfaces of PsbO, PsbU, and PsbV subunits contacting in the lumenal side to the adjacent PSII dimer in the crystal packing are around 45, 45, and 35 Å, respectively, and those in the B-monomer to the surfaces of PsbO and PsbU are 45 and 45 Å, respectively), but may be sufficient to change the OEC structures. This might be reflecting the highly fragile nature of the OEC. On the other hand, it should be pointed out that the temperature factors of the OECs tended to be slightly larger in the B-monomer than those in the A-monomer as listed in Table S5. This may be relating to the packing difference of the two monomers in the asymmetric unit. Nevertheless, the two different structures forced us to reconsider the assumption that the two monomers in the crystal exist in the same S_1-state of the Kok cycle. Hereafter, we assume two cases that the two monomers are (1) in the same S-state or (2) in different S-states. The S-state valences of the OECs are not restricted to integers in the crystals of PSII, because there remains a possibility that the OECs for the two monomers are the mixtures of S_1- and S_0-states to some extents. In general, the dark-stable PSII sample has been discussed as a mixture of 75% of S_1-state and 25% of S_0-state assuming that the S_0-, S_1-, S_2-, and S_3-states in the Kok cycle possess equal populations (the transient S_4-state is expected to have a very small population) and the S_2- and S_3-states return rapidly to the S_1-state. The S_1:S_0 ratio of 3:1 in the OECs will be changed if the populations of the four states from S_0 to S_3 are determined experimentally in the Kok cycle. Furthermore, because the PSII crystals are grown in the long incubation over 1 week at 12 °C (see Supporting Information), the S_1:S_0 ratio of the A- and B-monomers in the crystal might be altered through a very slow electron transfer reaction between the two monomers.

On the assumption (1), the OECs will be stabilized in the different structures, as shown in Figure 2. Mechanisms for oxygen evolution by the OEC have been proposed so far based on EXAFS studies,[11,18] XFEL structural analyses,[15] EPR studies,[19,20] and DFT computational calculations.[21,22] Most of the proposed mechanisms are based on the assumption that each of the S_1-, S_3-, S_4-, and S_0-states in the Kok cycle has a single structure. The exceptions are the mechanism proposed recently in which two components are included in the S_2- and S_3-states[20] or in the S_0-, S_1-, S_2-, and S_3-states.[22]

On the assumption (2), the S-state valences for the OECs of the A- and B-monomers are different, for example that the OECs are near to the S_1-state in the A-monomer and to S_0-state in the B-monomer, respectively. Saito et al.[17] have proposed a proton transfer mechanism from O4 to the lumenal bulk water region in the S_0-S_1 transition of the Kok cycle, based on the short hydrogen-bond distance between O4 and W6 in the crystal structure of 3ARC.[7] They suggested the low-barrier or single-well hydrogen bond between O4 and W6 in the S_0-state from theoretical calculations. The short length of the hydrogen bond between O4 and W6 in the B-monomer (2.44 Å), found in this study, can be explained by W6 being protonated as H_3O^+ and O4 being pulled strongly via electrostatic interactions. The corresponding O4−W6 distance in the A-monomer (2.66 Å) is normal as the usual hydrogen bonds, indicating that the proton on W6 is already released to the bulk water region. In our case, we should explain independently the hydrogen-bond distances between O3 and D1-His337 in the A-monomer (2.46 Å) and in the B-monomer (2.75 Å). D1-His337 can be speculated to be protonated as the positive His-H^+ residue in the A-monomer and be deprotonated as the neutral His residue in the B-monomer. The protonation of D1-His337 has been previously assumed in the computational study,[13] and another mechanism of proton transfer might be possible in the S_1−S_2 transition from O3 to a hydrogen-bond network of water molecules via D1-His337, although there is no crystal structure information for the S_2-state. The hydrogen-bond network includes Cl^-2, one of two chloride ions near the OEC (see Figure 4c in the previous report[7]). D1-His337 possibly transfers a proton to the hydrogen-bond network in cooperation with a quick rotation of the imidazole moiety around the Cα−Cβ bond, and Cl^-2 works as a proton acceptor. In this case, however, the proton reaching Cl^-2 would not be released to the lumenal bulk region because no release of protons is observed from PSII in the S_1−S_2 transition. If this kind of proton transfer mechanism is real, the hydrogen-bond network will act as a temporary storage of proton in the S_1−S_2 transition. Finally, if the valence number for the OEC could be different by two for the same S-state, the different structures of the OECs elucidated in this study might relate to discrepancies between the high- and low-oxidation state paradigms.[23]

In conclusion, X-ray reduction effects on the OEC structure have a threshold at a radiation dose below 0.12 MGy. The OEC structures determined in this study are slightly different from

DOI: 10.1021/jacs.6b09666
J. Am. Chem. Soc. 2017, 139, 1718−1721

the XFEL "radiation-damage-free" structures especially at the temperature factors of Ca atoms. The two monomers in the asymmetric unit in the PSII crystal exhibited two different structures of the OEC. There remain at present two possibilities for the S-state valences of the OECs in the two monomers in the asymmetric unit of the crystal, which are the same or different. The oxygen-evolving mechanism of PSII will be proposed on the structural information reported here. The real valences for the Mn atoms in the OECs in the PSII crystal should be elucidated by further studies in the near future.

■ ASSOCIATED CONTENT

Supporting Information

The Supporting Information is available free of charge on the ACS Publications website at DOI: 10.1021/jacs.6b09666.

Definition of PSII subunits and two monomers in the crystallographic asymmetric unit, measurements of Mn K-absorption edge profiles of PSII crystals, diffraction intensity measurements, and structure analyses (PDF)

■ AUTHOR INFORMATION

Corresponding Author

*nkamiya@sci.osaka-cu.ac.jp

ORCID

Nobuo Kamiya: 0000-0002-9056-7558

Funding

This work was supported by JSPS KAKENHI Grants No. 24227002 and partially by a Grant-in-Aid for Scientific Research on Innovative Areas "Artificial photosynthesis (AnApple) (No. 2406)", No. 24107003.

Notes

The authors declare no competing financial interest.

■ ACKNOWLEDGMENTS

X-ray diffraction datasets were obtained at beamlines BL38B1 and BL44XU of SPring-8. We thank Seiki Baba, Nobuhiro Mizuno, and Eiki Yamashita for their help in using the beamlines. (Proposal numbers: 2011B6613, 2012A6713, 2012B6713, 2013A6814, 2013B6814, 2014A6916, 2014B6916, 2015A1118, 2015A6512, 2015B6512.) X-ray absorption-edge profiles of PSII crystals were measured at BL26B1 of SPring-8. We thank Hideo Okumura and Yuki Nakamura for their help in the measurements. (Proposal numbers: 2015B1045, 2016A2576.) Atomic coordinates have been deposited in the Protein Data Bank under the accession numbers 5B5E and 5B66.

■ REFERENCES

(1) Kok, B.; Forbush, B.; McGloin, M. *Photochem. Photobiol.* **1970**, *11*, 457−475.
(2) Joliot, P. *Photosynth. Res.* **2003**, *76*, 65−72.
(3) Zouni, A.; Witt, H. T.; Kern, J.; Fromme, P.; Krauss, N.; Saenger, W.; Orth, P. *Nature* **2001**, *409*, 739−743.
(4) Kamiya, N.; Shen, J.-R. *Proc. Natl. Acad. Sci. U. S. A.* **2003**, *100*, 98−103.
(5) Ferreira, K. N.; Iverson, T. M.; Maghlaoui, K.; Barber, J.; Iwata, S. *Science* **2004**, *303*, 1831−1838.
(6) Guskov, A.; Kern, J.; Gabdulkhakov, A.; Broser, M.; Zouni, A.; Saenger, W. *Nat. Struct. Mol. Biol.* **2009**, *16*, 334−342.
(7) Umena, Y.; Kawakami, K.; Shen, J.-R.; Kamiya, N. *Nature* **2011**, *473*, 55−60.
(8) Kawakami, K.; Umena, Y.; Kamiya, N.; Shen, J.-R. *J. Photochem. Photobiol., B* **2011**, *104*, 9−18.
(9) Yano, J.; Kern, J.; Irrgang, K. D.; Latimer, M. J.; Bergmann, U.; Glatzel, P.; Pushkar, Y.; Biesiadka, J.; Loll, B.; Sauer, K.; Messinger, J.; Zouni, A.; Yachandra, V. K. *Proc. Natl. Acad. Sci. U. S. A.* **2005**, *102*, 12047−12052.
(10) Yano, J.; Kern, J.; Sauer, K.; Latimer, M. J.; Pushkar, Y.; Biesiadka, J.; Loll, B.; Saenger, W.; Messinger, J.; Zouni, A.; Yachandra, V. K. *Science* **2006**, *314*, 821−825.
(11) Glockner, C.; Kern, J.; Broser, M.; Zouni, A.; Yachandra, V.; Yano, J. *J. Biol. Chem.* **2013**, *288*, 22607−22620.
(12) Grabolle, M.; Haumann, M.; Muller, C.; Liebisch, P.; Dau, H. *J. Biol. Chem.* **2006**, *281*, 4580−4588.
(13) Galstyan, A.; Robertazzi, A.; Knapp, W. *J. Am. Chem. Soc.* **2012**, *134*, 7442−7449.
(14) Luber, S.; Rivalta, I.; Umena, Y.; Kawakami, K.; Shen, J.-R.; Kamiya, N.; Brudvig, G. W.; Batista, V. S. *Biochemistry* **2011**, *50*, 6308−6311.
(15) Suga, M.; Akita, F.; Hirata, K.; Ueno, G.; Murakami, H.; Nakajima, Y.; Shimizu, T.; Yamashita, K.; Yamamoto, M.; Ago, H.; Shen, J.-R. *Nature* **2015**, *517*, 99−103.
(16) Askerka, M.; Vinyard, D. J.; Wang, J.; Brudvig, G. W.; Batista, V. S. *Biochemistry* **2015**, *54*, 1713−1716.
(17) Saito, K.; Rutherford, A. W.; Ishikita, H. *Nat. Commun.* **2015**, *6*, 8488.
(18) Dau, H.; Grundmeier, A.; Loja, P.; Haumann, M. *Philos. Trans. R. Soc., B* **2008**, *363*, 1237−1243.
(19) Cox, N.; Retegan, M.; Neese, F.; Pantazis, D. A.; Boussac, A.; Lubitz, W. *Science* **2014**, *345*, 804−808.
(20) Boussac, A.; Rutherford, A. W.; Sugiura, M. *Biochim. Biophys. Acta, Bioenerg.* **2015**, *1847*, 576−586.
(21) Siegbahn, P. E. *Biochim. Biophys. Acta, Bioenerg.* **2013**, *1827*, 1003−1019.
(22) Shoji, M.; Isobe, H.; Nakajima, T.; Yamaguchi, K. *Chem. Phys. Lett.* **2016**, *658*, 354−363.
(23) Petrie, S.; Pace, R. J.; Stranger, R. *Angew. Chem., Int. Ed.* **2015**, *54*, 7120.

DOI: 10.1021/jacs.6b09666
J. Am. Chem. Soc. 2017, 139, 1718−1721